

Article

# Noise Emission of a 200 kW Vertical Axis Wind Turbine

Erik Möllerström <sup>1,2,\*</sup>, Fredric Ottermo <sup>1</sup>, Jonny Hylander <sup>1</sup> and Hans Bernhoff <sup>2</sup>

Received: 31 October 2015; Accepted: 22 December 2015; Published: 29 December 2015

Academic Editor: Frede Blaabjerg

<sup>1</sup> School of Business, Engineering and Science, Halmstad University, Halmstad SE-301 18, Sweden; fredric.ottermo@hh.se (F.O.); jonny.hyllander@hh.se (J.H.)

<sup>2</sup> Division for Electricity, Department of Engineering Sciences, Uppsala University, Uppsala SE-751 21, Sweden; hans.bernhoff@angstrom.uu.se

\* Correspondence: erik.mollerstrom@hh.se; Tel.: +46-35-16-7971; Fax: +46-35-18-6192

**Abstract:** The noise emission from a vertical axis wind turbine (VAWT) has been investigated. A noise measurement campaign on a 200 kW straight-bladed VAWT has been conducted, and the result has been compared to a semi-empirical model for turbulent-boundary-layer trailing edge (TBL-TE) noise. The noise emission from the wind turbine was measured, at wind speed 8 m/s, 10 m above ground, to 96.2 dBA. At this wind speed, the turbine was stalling as it was run at a tip speed lower than optimal due to constructional constraints. The noise emission at a wind speed of 6 m/s, 10 m above ground was measured while operating at optimum tip speed and was found to be 94.1 dBA. A comparison with similar size horizontal axis wind turbines (HAWTs) indicates a noise emission at the absolute bottom of the range. Furthermore, it is clear from the analysis that the turbulent-boundary-layer trailing-edge noise, as modeled here, is much lower than the measured levels, which suggests that other mechanisms are likely to be important, such as inflow turbulence.

**Keywords:** vertical axis wind turbine (VAWT); H-rotor; noise; noise emission; sound power level

## 1. Introduction

Wind turbines are categorized into two groups by the orientation of their axis of rotation: horizontal axis wind turbines (HAWTs) and vertical axis wind turbines (VAWTs). The HAWT has by far been the most successful concept, with the large and economically feasible turbines of today; however, the VAWT concept has some advantages. VAWTs typically have fewer moving parts and a generator located at ground level which could ultimately lead to higher availability and lower maintenance cost [1]. Furthermore, it has been shown that the concept is more suitable for up-scaling than the HAWT concept [2]. Moreover, of special interest here, VAWTs has potentially lower noise emission [1].

Noise is considered as one of the disadvantages with wind turbines and noise levels at dwellings and other sensitive areas are typically regulated in national legislation which restrains potential locations for wind turbines. For example, in Sweden the recommendations for wind turbine noise are set by the Swedish Environmental Protection Agency (SEPA) [3] to 40 dBA at dwellings, which are further lowered to 35 dBA if obvious tones are present in the spectrum. A limit of 35 dBA is set for specifically sensitive areas such as natural parks and planned recreational areas. These limits are based on the sound intensity created at a wind speed of 8 m/s, 10 m above ground and measured over 4 h. The definition of noise is simply unwanted sound [4]. Distinguishing noise from sound is to a large extent subjective, but sound from wind turbines is generally considered as unwanted and may therefore be referred to as noise.

Extensive research has been presented regarding noise from wind turbines. For example, in [5] the sound modeling, masking and propagation has been studied and in [6] the human response to

wind turbine noise has been investigated. However, most research has been concentrated towards the more common HAWT concept whereas little attention has been given to the alternative VAWT, which has shown potential for lower noise levels. Work that has been done regarding noise from VAWTs includes [7,8] where numerical methods are used to simulate aerodynamic noise from VAWTs and which for both studies indicate lower noise levels compared to HAWTs. In [9] the noise characteristics of a model VAWT were investigated and the applicability of different noise prediction models was examined. Simulations of VAWT noise emissions from first principles would require an accurate determination of the flow close to the blade, which is a computationally expensive task. However, recent progress with large eddy simulations [10–14] might render this approach feasible further on.

In this paper, the noise emission from a 200 kW VAWT is investigated, both by experiments and by using a semi-empirical noise model. Experimental results are compared to the noise emissions of similar sized HAWTs and also used to compare with simple noise modeling, enabling conclusions to be drawn regarding the applicability of the model for a medium sized VAWT.

## 2. Theory

Noise from operating wind turbines can be divided into aerodynamic and mechanical noise. Aerodynamic noise is of broadband character, it occurs when the air flows around the blade and originates from various complex flow phenomena. The generated noise generally increases with tip speed and hence the most sound is produced at or close to the tip of the blade. Mechanical noise originates from the relative motions of mechanical components in the gearbox, the generator, yaw drives, cooling fans, hydraulics, and power electronics. For modern turbines the aerodynamic noise is generally dominant and in [15] it is shown that for a modern HAWT the most noise is created close to the blade tip when the blade travels downwards towards the receiver, a result of the directivity of aerodynamic noise emitted from a moving airfoil [4]. The characteristically swishing sound of a wind turbine is due to amplitude modulation and has been proven to be the sound feature from wind turbines that is the most annoying [4]. This mid frequency phenomena (400–1000 Hz) is created by the directivity of the trailing edge noise, and convective amplification. The effect of amplitude modulation will not be further discussed in this work as we will be focusing on the averaged level of the aerodynamic noise.

VAWTs usually have lower tip speed ratios (TSR) than HAWTs. The entire length of a VAWT blade travels at tip speed, which for a HAWT is only true for the actual blade tip. Since it has been shown that most of the aerodynamic noise from a HAWT is generated close to the tip [15], lower levels of aerodynamic noise might be expected for a VAWT due to the relatively low blade velocity compared with the case of a HAWT. However, the reality is likely to be more complex. An important difference is that the blades of a VAWT experience a varying angle of attack, whereas for the HAWT case, the angle of attack is nearly constant. An additional difference is that VAWTs usually have support arms carrying the blades, a feature not needed for HAWTs. However, the support arms can be made streamlined, in which case they will not be expected to generate much noise. Furthermore, the VAWT drive train can be located at ground level which limits mechanical noise propagation [1].

### *Modeling the Noise*

It has been demonstrated that noise from modern HAWTs is well modeled by the turbulent-boundary-layer trailing edge (TBL-TE) noise contribution [15]. Guided by this, we try to estimate the noise level by using the empirical model for airfoil self-noise in [16], in particular the TBL-TE part of this model. For small VAWTs (low Reynolds numbers) laminar-boundary-layer trailing edge noise has been observed to be important [9], but for the larger-sized turbine considered here the Reynolds number is of the order of  $1 \times 10^6$ , so the TBL-TE is expected to be dominant over the laminar-boundary-layer part. A complication is that the model in [16] assumes static angles of attack, whereas in this case the angle of attack is constantly changing. However, static angle-of-attack lift

and drag data has been successfully used in prediction models of VAWT performance [17], so it is reasonable to evaluate a static approach here as well.

A rapidly varying angle of attack gives rise to a dynamic stall effect, which means that flow separation at large angles of attack is effectively delayed. In [9], it was observed that the dynamic stall effect seems to constitute a measurable source of noise, probably due to large force fluctuations when the flow eventually separates. This was however only observed for very low TSRs, indicating that strong flow separation will not occur for TSR values in the range 2.9 to 3.8, as considered here. In [18], different models for dynamic stall was applied to a VAWT for TSR values between 2.20 and 3.09, and dynamic stall is seen to be present even at TSR 3.09, but its effect here seems to be that stall is to a large extent avoided. Thus we can expect that the TBL-TE noise might be somewhat overestimated using a static model for the current TSR range, as the airfoil is stalling less in reality due to dynamic stall.

When calculating the angles of attack, a simple model is adopted, where the flow is assumed to be unperturbed by the turbine, and the angles of attack range up to  $15^\circ$ , hence reaching the stall region. More sophisticated flow models will halt the flow around the turbine, implying slightly lower angles of attack. In reality the VAWT flow is very complex and difficult to simulate accurately, so the actual angle of attack in this situation is a source of uncertainty. However, to get an indication of the noise levels produced by the TBL-TE model of [16] it seems reasonable to use the simple approach presented here.

The basic empirical equation for the sound pressure spectrum due to the TBL-TE noise for an airfoil [15,16] is:

$$p^2(f) = K(f) \frac{\delta^* M^5 L}{R^2} \cdot \frac{2 \sin^2(\theta/2) \sin^2 \varphi}{(1 - M \cos \xi)^4} \quad (1)$$

where  $K(f)$  is a frequency dependent constant,  $\delta^*$  is the displacement thickness of the boundary layer at the trailing edge,  $M$  is the blade Mach number,  $L$  is the blade span and  $R$  the distance from the source to the observer. The angles  $\theta$ ,  $\varphi$  and  $\xi$  are defined according to [15], illustrated for the current geometry in Figure 1.  $\theta$  is the angle between the source-observer line and the blade chord line,  $\xi$  is the angle between the source-observer line and the relative wind speed, and  $\varphi$  is understood from Figure 1. When calculating  $R$  and the angles, the motion of the air flow needs to be taken into account, using retarded coordinates for the source. In the current geometry, however, this is easily achieved by simply offset the observer position according to the wind speed and sound travel time. The procedure for calculating  $K(f)$  is given in [16] for 1/3 octave bands; the calculation involves the Strouhal number corresponding to the displacement thickness and lengthy parametrizations of experimental observations. There are three contributions to  $p^2$ , one from the suction side, one from the pressure side and one additional term due to the angle of attack. Each of these contributions has a separate calculation of the displacement thickness and the frequency dependence.

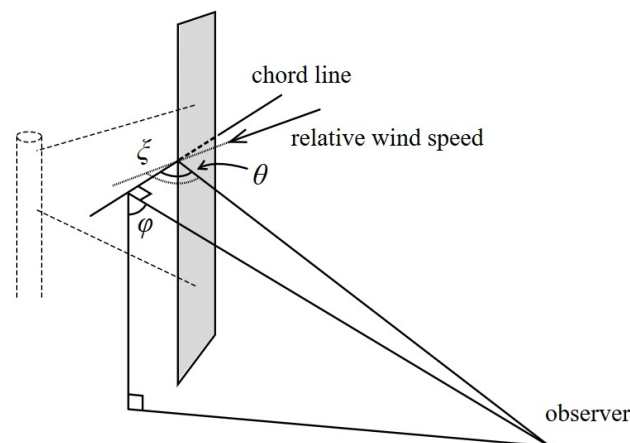


Figure 1. Definition of the angles  $\theta$ ,  $\varphi$  and  $\xi$ .

Positioning the observer downwind at a certain horizontal distance  $R_h$  to the hub, the angles  $\theta$ ,  $\varphi$  and  $\xi$ , and source-observer distance  $R$ , are determined as a function of the turbine dimensions and the blade azimuth angle  $\beta$ . The squared pressure of Equation (1) is then averaged over the angles  $\beta$  and multiplied by 3 (three blades). Finally, the A-weighted sound pressure level is calculated.

### 3. Method

#### 3.1. Wind Turbine System

The VAWT we consider in this study is a so called H-rotor, which is a Darrieus-type [19] turbine with straight fixed blades. A 200 kW VAWT (hereafter referred to as the T1-turbine) was designed and erected in 2010 by the Company Vertical Wind AB (Uppsala, Sweden) in collaboration with Uppsala University (Uppsala, Sweden). Only one 200 kW turbine was ever built by vertical wind AB, making the T1-turbine unique. The turbine, which is located at Thorsholm ( $56^{\circ}56'29''\text{N}$ ,  $12^{\circ}30'38''\text{E}$ ) just outside of Falkenberg at the west coast of Sweden, is today owned by Uppsala University and it is the subject of research in a variety of fields [20–23]. The T1-turbine has a direct drive permanent magnet synchronous generator mounted at the bottom of the tower and connected to the rotor by a steel shaft. The rotor consists of three 24 m long straight blades that are connected to the shaft by two struts each. Both blades and struts are made out of fiberglass. The blades are fixed, but the variable speed of the turbine is used to control the stall effect so that the rated power can be attained between the rated wind speed and the cut-out wind speed.

The T1-turbine has a tower made out of laminated wood, which from the start was free standing, but after two years was complemented with support from three guy-wires. The effect of the guy-wires on the tower dynamics has been examined in [20].

The T1-turbine is a first prototype and the noise level was not considered during design. It is reasonable to assume that the noise level could be further reduced, for example by altering the blade shape and choosing a blade profile developed to minimize noise. However, the standard NACA0018 blade profile used for the T1-turbine allows for straightforward use of existing experimental data on noise generation.

The T1-turbine and its properties can be seen in Figure 2 and Table 1.



Figure 2. The T1-turbine.

**Table 1.** Properties of the T1-turbine.

Category	Property	Value
Operation	Rated power	200 kW
	Rotational speed	16–33 rpm
	Nominal tip speed ratio	3.8
	Cut-in wind speed	4 m/s
	Rated wind speed	12 m/s
	Cut-out wind speed	25 m/s
	Survival wind speed	60 m/s
	Power regulation	Stall
Geometry	Turbine diameter	26 m
	Hub height (foundation included)	40 m
	Blade length	24 m
	Blade chord	0.4–0.9 m
	Swept area	624 m <sup>2</sup>
Material	Blade/strut material	Fiberglass composite
	Tower material	Laminated wood

### 3.2. Experimental Setup

The microphone used was a BSWA MP201 which together with preamplifier MA211 gives a flat frequency response and Class 1 accuracy (<0.7 dBA) according to the international standard for sound level meters, IEC61672-1 [24]. A Norsonic Nor140 was used as field recorder. For calibration an acoustic calibrator, Brüel and Kjær type 4231, was used. For setting the distance to the tower a laser rangefinder, Leica Pinmaster, with an accuracy of  $\pm 1$  m, was used.

For recording the sound pressure level of the wind turbine, the microphone was mounted on an acoustically hard circular board with a primary 90 mm and a secondary 250 mm wind protection. The circular board gives a coherent addition  $c = 6$  dB. The total acoustic attenuation of the wind protections is 0.5 dB with the largest effect on higher frequencies, this effect is deemed negligible and has not been accounted for in the result. The entire setup is consistent with the international standard International Electrotechnical Commission 61400-11 “Wind turbines—Part 11: Acoustic noise measurement techniques” [25].

The wind speed was measured by a Thies Clima 4.3351.00.161 cup anemometer, placed at a height of 42 m on a wind measurement mast situated 100 m from the actual turbine. The anemometer has a measuring instability of <1% or <0.2 m/s. The signals from the anemometer was measured by a PLC (programmable logic controller; model: Millenium 3 XD26, Crouzet, San Diego, CA, USA) and logged, at a sampling frequency of 1 Hz, by the cRIO (CompactRIO; model: cRIO9074, National Instruments, Austin, TX, USA) belonging to the wind turbine control system. The rotational speed of the T1-turbine was measured by a 10-bit rotational encoder which was placed on the lower end of the drive shaft. The rotational speed was logged by the same cRIO as the wind speed.

### 3.3. Observations

The T1-turbine is located in a plain field with a heavy trafficked motorway 750 m to its southwest. Interfering noise from this freeway was evened out due to the distance and was approximately at the same level during the entire recording. Furthermore there is a farm located nearby with its access road just 70 m from the turbine but there were no interfering traffic during the time of recording. The microphone was placed at a distance of  $R_h = 40$  m from the tower.

### 3.4. Calculating Noise Emission from Recordings

When recording noise from a wind turbine, the sound recorded  $L_{p,rec}$  (in dBA) consists of the sound pressure level due to the wind turbine noise  $L_{p,wt}$  as well as the background sound  $L_{p,bg}$  which are related by [4]:

$$L_{p,rec} = 10 \cdot \log_{10}(10^{L_{p,wt}/10} + 10^{L_{p,bg}/10}) \quad (2)$$

Recording with the wind turbine sequentially turned on and shut down and assuming that the wind and background sound conditions are unchanged, Equation (2) can be used to separate the wind turbine sound pressure level from the total sound pressure level. In reality, the conditions are never unchanged. But by keeping track on the wind speed and using long enough recordings, the effect of wind speed can be taken into account and the effect of background sound conditions will be evened out. The emitted sound pressure levels of the wind turbine and background can, by taking the spherical sound distribution and the coherent addition of sound reflected from the ground  $c$ , be used to calculate the emitted sound power level (hereafter called noise emission)  $L_{W,wt}$  (in dBA) of the wind turbine by:

$$L_{W,wt} = L_{p,wt} - c + 10 \cdot \log_{10} \left( \frac{4\pi R^2}{S_0} \right) \quad (3)$$

where  $S_0$  is a reference area of  $1 \text{ m}^2$  and  $R = \sqrt{R_h^2 + H^2}$  is the distance between the rotor axis at hub height and the place of recording, where  $H$  is the hub height of the turbine and  $R_h$  the horizontal distance between tower and place of recording. The standardized measurement procedure for deciding the noise emission is described in the standard [25] and a similar but not identical approach has been used for this work.

#### Method of Bins and Standard Uncertainty

To calculate the noise emission for a certain wind speed,  $L_{p,wt}$  and  $L_{p,bg}$  must be quantified for that wind speed. For this, the IEC standard specifies using the method of bins. The measured data, presented as 10 s mean values, is divided into bins, *i.e.* uniformly sized sections along the wind speed axis. After that, the mean values of the sound pressure level  $\bar{L}_{p,i}$  and the mean wind speed  $\bar{V}_i$ , for bin  $i$ , are calculated as:

$$\bar{L}_{p,i} = 10 \cdot \log_{10} \left( \frac{1}{N_i} \sum_{j=1}^{N_i} 10^{\left(\frac{L_{p,i,j}}{10}\right)} \right) \quad (4)$$

$$\bar{V}_i = \frac{1}{N_i} \sum_{j=1}^{N_i} v_{i,j} \quad (5)$$

where  $L_{p,i,j}$  and  $v_{i,j}$  is the sound pressure level and wind speed at measurement period  $j$  in bin  $i$ , and  $N_i$  is the number of measurement periods. The sound pressure level at wind speeds not coinciding with  $\bar{V}_i$  is obtained by linear interpolation of the mean bin values. This is done for the wind turbine noise data to get  $L_{p,wt}$ , and for the background data to get  $L_{p,bg}$ .

The calculation of the standard uncertainties follows the prescription in the IEC standard. The standard uncertainty for  $\bar{L}_{p,i}$  is calculated as:

$$u_{L_{pi}} = \sqrt{\frac{\sigma_{L_{pi}}^2}{N_i} + u_{L_{pe}}^2} \quad (6)$$

where  $\sigma_{L_{pi}}$  is the standard deviation of  $\bar{L}_{p,i}$  for bin  $i$ , and  $u_{L_{pe}}$  is the overall precision of the corresponding measurement equipment. The next step is to obtain the standard uncertainties at the interpolated positions, for which the uncertainty of the wind speed is also needed (calculated

analogously to Equation (6)), as well as the covariance of the wind speed and the sound pressure level. See [25] for details.

### 3.5. Measurement Limitations

According to the standard [25], regarding VAWTs, a distance  $R_h = H + D$  should be used between the measuring point and the turbine, where  $H$  is the hub height and  $D$  the equatorial rotor diameter. A 20% or maximum 30 m deviation is allowed as long as the distance is measured with an accuracy of  $\pm 2\%$ . However, in this study, a distance  $R_h = H$  was used, which is below the minimum distance allowed for VAWTs. The distance  $R_h = H + D$  appears reasonable for guy-wired Darrieus-type VAWTs (the historically most common type), where hub heights are generally low. The specified HAWT distance,  $R_h = H + D/2$ , would in the Darrieus case imply a measurement point very close to the blade. The VAWT studied here, with its high tower, is in this sense, however, more similar to a HAWT. In addition, the relatively high noise level due to the nearby freeway motivated a measurement point even a little closer, at  $R_h = H$ , to increase signal to noise ratio.

The measurements were performed with an upper limit of the rotational speed set to 22 rpm. The reason for this is that the added guy-wires stiffen the tower so that the first mode Eigen frequency of the tower is excited at 23 rpm. The limitation means that the turbine was operated at optimum tip speed for the measurements done at 6 m/s (10 m height) but for higher wind speeds the tip speed was below optimum and thus the turbine was stalling. The stalling contributes to the creation of noise while the lower velocity of the blade counteracts it [4]. It is unclear which effect is most important.

## 4. Results

A recording was performed with the turbine first turned on for 60 min, then turned off for 24 min and then turned on again for another 11 min. The mean wind speed at hub height was 8.0 m/s and 9.5 m/s with the turbine turned on and off respectively. If recalculated to the standard 10 m height, using power law extrapolation described in [26], these wind speeds equals 6.3 m/s and 7.4 m/s. By using the 10 s based mean values and assuming that the turbine is turned off when the electric output is below 5% of rated power, the total and background noise can respectively be presented as functions of wind speed, see Figure 3. Using the linear relations between the mean bin values from Figure 3 together with Equation (2), the wind turbine sound pressure level  $L_{p,wt}$  can be decided for different wind speeds. Thereafter, the noise emission  $L_{W,wt}$  can be decided with Equation (3). The noise emissions with standard uncertainty for wind speeds between 5 m/s and 8 m/s are displayed in Table 2.

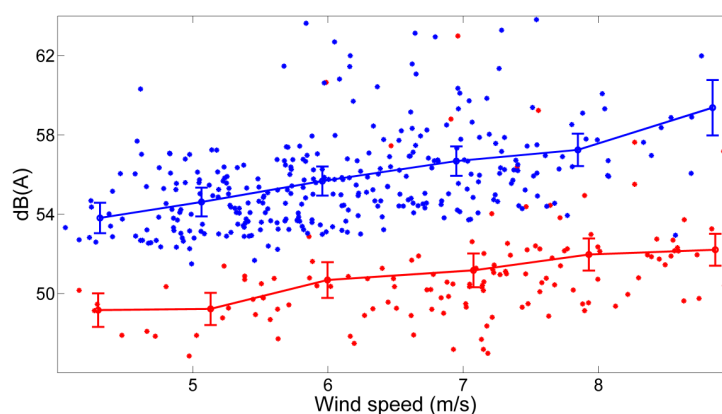


**Figure 3.** Sound pressure level against wind speed (recalculated to 10 m above ground) presented as an average per 10 s with turbine turned on (blue) and off (red). The standard uncertainty is plotted for the sound pressure levels for each bin.

**Table 2.** Noise emission for different wind speeds calculated from results of recordings.

Wind Speed at 10 m Height	Tip Speed Ratios (TSR)	Noise Emission with Standard Uncertainty	Noise Model Calculation
m/s	-	dBA	dBA
5	3.8	$93.1 \pm 1.0$	69.6
6	3.8	$94.1 \pm 1.1$	74.5
7	3.4	$95.4 \pm 1.0$	78.6
8	2.9	$96.2 \pm 1.0$	82.3

In Figure 4, the 1/3 octave band of the wind turbine noise can be seen. These bands correspond to the sound pressure level, from the wind turbine, at the recording distance and a hub height wind speed of 8.0 m/s. Each of the bands is calculated using the same method as described for  $L_{p,wt}$  above.

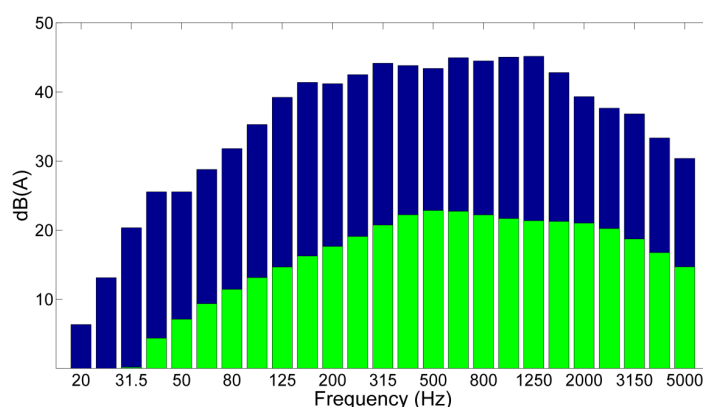


**Figure 4.** 1/3 octave band of T1-turbine sound pressure level: experimental (blue) and modeled (green). Both cases for a wind speed (hub height) of 8.0 m/s.

Also shown in Figure 4 is the resulting spectrum of the TBL-TE noise calculation outlined in Section 2. Conforming to the experimental setup, a horizontal recording distance of 40 m and mean wind speed of 8.0 m/s at hub height has been used. Input values for the turbine geometry and TSR are the ones given in Table 1, however with a constant chord length of 0.8 m. Even if the form of the spectrum shows resemblance with the measured one, it can be clearly seen that the calculated noise levels are well below what is measured. The overall calculated emission level is 15–20 dB lower, as can be seen in Table 2. This suggests that the TBL-TE noise, as modeled here, is not alone responsible for the measured noise. As seen in the Table 2, however, the difference decreases for higher wind speeds. This decrease could perhaps be attributed to the static stall of the TBL-TE model; at lower TSR the airfoil reaches deeper into the stall region and assuming fully developed static stall at all times within this region is likely to imply a higher noise level than if dynamic stall is present, as discussed in Section 2 above.

## 5. Discussion and Conclusions

The noise emission of the T1-turbine at 8 m/s, 10 m above ground, was measured to 96.2 dBA. At this wind speed the turbine was stalling due to the upper limit of the rotational speed added after installing the guy wires, and the effect of this upon the noise level is unclear as there are two balancing effects. The noise emission at 6 m/s 10 m above ground was measured to 94.1 dBA, this while operating at optimum tip speed. Available noise surveys performed on similar sized HAWTs [27–30] has established noise emissions of 95.1–100.2 dBA and 97.3–102.4 dBA for 6 m/s and 8 m/s respectively, see Table 3 for details. Using this for comparison, the T1-turbine indicates a noise emission at the

absolute lower range of the similar size HAWTs while running at optimum tip speed. At 8 m/s the noise emission of the T1-turbine is still lower than any of the compared HAWTs.

**Table 3.** Noise emission and specifications of horizontal axis wind turbines (HAWTs) in comparison. Wind speeds for noise emissions are stated for 10 m above ground [27–30].

Turbine Model	Power (kW)	Rotor Diameter (m)	No. of Blades	Power Regulation	dBA at 6 m/s	dBA at 8 m/s
Vestas V27	225	27	3	Pitch	96.7	97.3
GEV-MP R	200–275	32	2	Pitch	100.2	102.4
WTN250	250	30	3	Stall	95.1	99.8
Norwin 29/225	225	29	3	Stall	95.2	97.5

The noise emission of the VAWT is not properly modeled by the TBL-TE part of the airfoil self-noise model given in [16]. This suggests that other mechanisms are important for understanding noise generation on VAWTs of this size. In [9], where a small VAWT is studied, it was anticipated that the inflow turbulence is responsible for generating most of the noise, and the TBL-TE noise was found to be about 15 dB lower than the measured value. It is interesting to note that an equal deviation is found here, in spite of the substantial difference in size. If the noise from a MW-size VAWT is believed to be dominated by the TBL-TE noise, as seems to be the case for modern MW-size HAWTs, one would have expected the TBL-TE noise calculation to more closely reproduce the measured values for this intermediate-size VAWT. Using a model intended for a steady angle of attack in a context where the angle of attack varies will naturally lead to deviations, but as long as the stall region is not entered, and dynamic stall is not prominent, the deviations are likely to be much smaller than 15 dB. Still, to accurately assess the TBL-TE contribution for VAWTs one would need models that properly address the unsteady angle of attack.

The noise characteristics of VAWTs need to be investigated further and the 200 kW T1-turbine creates an opportunity doing so utilizing perhaps the largest operational VAWT existing today. Examples of future work on the T1-turbine are noise directivity measurements, amplitude modulation analysis and quantification of the aerodynamic noise sources using a microphone array.

**Acknowledgments:** This work was conducted within the STandUP for ENERGY strategic research framework. Vertical Wind AB is acknowledged for further financial support.

**Author Contributions:** Erik Möllerström analyzed the experimental measurements, helped with noise modeling and wrote most of the article. Fredric Ottermo was main responsible for noise modeling and wrote parts of the article. Jonny Hylander and Hans Bernhoff supervised the project.

**Conflicts of Interest:** The authors declare no conflict of interest.

## References

1. Eriksson, S.; Bernhoff, H.; Leijon, M. Evaluation of different turbine concepts for wind power. *Renew. Sustain. Energy Rev.* **2008**, *12*, 1419–1434. [[CrossRef](#)]
2. Ottermo, F.; Bernhoff, H. An upper size of vertical axis wind turbines. *Wind Energy* **2013**, *17*, 1623–1629. [[CrossRef](#)]
3. Adolfsson, E. *Riktvärden för Ljud från Vindkraft*; Swedish Environmental Protection Agency: Stockholm, Sweden, 2010. (In Swedish)
4. Bowdler, D.; Leventhall, H.G. *Wind Turbine Noise*; Multi Science Publishing Company Limited: Hockley, UK, 2011.
5. Bolin, K. *Wind Turbine Noise and Natural Sounds: Masking, Propagation and Modeling*. Ph.D. Thesis, Royal Institute of Technology, Stockholm, Sweden, 2009.
6. Pedersen, E. *Human response to wind turbine noise: Perception, annoyance and moderating factors*. Ph.D. Thesis, The Sahlgrenska Academy, University of Gothenburg, Gothenburg, Sweden, 2007.
7. Iida, A.; Mizuno, A.; Fukudome, K. Numerical simulation of aerodynamic noise radiated from vertical axis wind turbines. In Proceedings of the 18 International Congress on Acoustics, Kyoto, Japan, 4–9 April 2004.

8. Dumitrescu, H.; Cardos, V.; Dumitrache, A.; Frunzulica, F. Low-frequency noise prediction of vertical axis wind turbines. *Proc. Rom. Acad.* **2010**, *11*, 47–54.
9. Pearson, C. Vertical axis wind turbine acoustics. Ph.D. Thesis, Cambridge University, Cambridge, UK, 2014.
10. Barsky, D.; Posa, A.; Rahromostaqim, M.; Leftwich, M.C.; Balaras, E. Experimental and computational wake characterization of a vertical axis wind turbine. In Proceedings of the 32nd AIAA Applied Aerodynamics Conference, Atlanta, GA, USA, 16–20 June 2014.
11. Elkhoury, M.; Kiwata, T.; Aoun, E. Experimental and numerical investigation of a three-dimensional vertical-axis wind turbine with variable-pitch. *J. Wind Eng. Ind. Aerodyn.* **2015**, *139*, 111–123. [[CrossRef](#)]
12. Li, C.; Zhu, S.; Xu, Y.; Xiao, Y. 2.5 D large eddy simulation of vertical axis wind turbine in consideration of high angle of attack flow. *Renew. Energy* **2013**, *51*, 317–330. [[CrossRef](#)]
13. Shamsoddin, S.; Porté-Agel, F. Large eddy simulation of vertical axis wind turbine wakes. *Energies* **2014**, *7*, 890–912. [[CrossRef](#)]
14. Ferreira, C.J.S.; van Zuijlen, A.; Bijl, H.; van Bussel, G.; van Kuik, G. Simulating dynamic stall in a two-dimensional vertical-axis wind turbine: Verification and validation with particle image velocimetry data. *Wind Energy* **2010**, *13*, 1–17. [[CrossRef](#)]
15. Oerlemans, S.; Sijtsma, P.; López, B.M. Location and quantification of noise sources on a wind turbine. *J. Sound Vib.* **2007**, *299*, 869–883. [[CrossRef](#)]
16. Brooks, T.F.; Pope, D.S.; Marcolini, M.A. *Airfoil Self-Noise and Prediction*; National Aeronautics and Space Administration: Hampton, VA, USA, 1989.
17. Paraschivoiu, I. *Wind Turbine Design: With Emphasis on Darrieus Concept*; Presses inter Polytechnique: Montreal, QC, Canada, 2002.
18. Dyachuk, E.; Goude, A. Simulating Dynamic Stall Effects for Vertical Axis Wind Turbines Applying a Double Multiple Streamtube Model. *Energies* **2015**, *8*, 1353–1372. [[CrossRef](#)]
19. Marie, D.G.J. Turbine Having Its Rotating Shaft Transverse to the Flow of the Current. U.S. Patent 1,835,018, 8 December 1931.
20. Möllerström, E.; Ottermo, F.; Hylander, J.; Bernhoff, H. Eigen Frequencies of A Vertical Axis Wind Turbine Tower Made of Laminated Wood and the Effect Upon Attaching Guy Wires. *Wind Eng.* **2014**, *38*, 277–290. [[CrossRef](#)]
21. Eriksson, S.; Kjellin, J.; Bernhoff, H. Tip Speed ratio control of a 200 kW VAWT with synchronous generator and variable DC voltage. *Energy Sci. Eng.* **2013**, *1*, 135–143. [[CrossRef](#)]
22. Kjellin, J.; Eriksson, S.; Bernhoff, H. Electric control substituting pitch control for large wind turbines. *J. Wind Energy* **2013**, *2013*. [[CrossRef](#)]
23. Möllerström, E.; Ottermo, F.; Goude, A.; Eriksson, S.; Hylander, J.; Bernhoff, H. Turbulence influence on wind energy extraction for a medium size vertical axis wind turbine. *Wind Energy* **2016**, in press.
24. *Electroacoustics—Sound Level Meters—Part 1: Specifications, Edition 2*; IEC 61672-1; The International Electrotechnical Commission (IEC): Genève, Switzerland, 2013.
25. *Wind Turbine Generator Systems—Part 11: Acoustic Noise Measurement Techniques, Edition 3*; IEC 61400-11; The International Electrotechnical Commission (IEC): Genève, Switzerland, 2012.
26. Manwell, J.F.; McGowan, J.G.; Rogers, A.L. *Wind Energy Explained: Theory, Design and Application*; John Wiley & Sons: Hoboken, NJ, USA, 2010.
27. Noise Measurement of VESTAS V27-225kW Wind Turbine, DNV Det Norske Veritas. Available online: <http://www.southhams.gov.uk/planningdocs/1/00/20/23/00202341.pdf> (accessed on 27 June 2014).
28. GEV MP-R32 m Rotor Diameter Sound Power Levels, VERGNET Wind Turbines. Available online: <http://www.cesa.org/assets/2013-Files/ITAC/VergnetGEVMPRacousticreport.pdf> (accessed on 23 July 2014).
29. Noise Assessment NORWIN 29 225 kW Wind Turbine, 24 Acoustics. Available online: <http://planning.allerdale.gov.uk/portal/servlets/AttachmentShowServlet?ImageName=218119> (accessed on 23 July 2014).
30. General Noise Specifications WTN 250 kW. Wind Technik Nord GmbH. Available online: <http://www.newport.gov.uk/stellent/groups/public/documents/planningdocument/cont616474.pdf> (accessed on 23 July 2014).

